Materials Science Forum Vol. 508 (2006) pp 431-436
Online available since 2006/Mar/15 at www.scientific.net

doi:10.4028/www.scientific.net/MSF.508.431

Phase-Field Modeling of Dendritic Solidification in Undercooled Droplets Processed by Electromagnetic Levitation

P.K. Galenko[1], D.M. Herlach, G. Phanikumar, O. Funke

Institute of Space Simulation, DLR, D-51170, Cologne, Germany

peter.galenko@dlr.de

Keywords: phase-field, solidification, forced convection, solute diffusion

Abstract. The results on modeling dendritic solidification from undercooled melts processed by the electromagnetic levitation technique are discussed. In order to model the details of formation of dendritic patterns we use a phase-field model of dendritic growth in a pure undercooled system with convection of the liquid phase. The predictions of the phase-field model are discussed referring to our latest high accuracy measurements of dendrite growth velocities in nickel samples. Special emphasis is given to the growth of dendrites at small and moderate undercoolings. At small undercoolings, the theoretical predictions deviate systematically from experimental data for solidification of nickel dendrites. It is shown that small amounts of impurities and forced convective flow can lead to an enhancement of the velocity of dendritic solidification at small undercoolings.

Introduction

Different techniques have been applied for measuring dendritic growth velocities during solidification of electromagnetically levitated melts, e.g. using a fast responding photo-double-diode [1] or an ultra-high-speed camera system [2]. The Lipton-Kurz-Trivedi (LKT) model of dendrite growth [3] predicts the dendrite growth velocity V as a function of the undercooling ΔT in good agreement with experimental data for nickel only in the region of medium undercoolings of 100 K < ΔT < 200 K (see Ref. [1]). Recently, we suggested a modification to the LKT model which takes into account the effect of forced convective flow caused by electromagnetic stirring [4]. The modified model predicts an increase of growth velocity when the flow is directed opposite to the dendrite growth. However, the effect of forced convective flow alone can still not explain the measured data satisfactorily [4]. An additional reason for dendrite velocities higher than predicted by the model might be the presence of small amounts of impurities which may drastically influence the kinetics of solidification [5]. Therefore we present phase-field model predictions in comparison with measurements of dendrite velocities. To test the influence of a small amount of impurities, the functions "velocity V-undercooling ΔT" are presented for Ni dendrites in comparison with a very dilute Ni alloy.

Equations of the model

We have used the phase-field model via "thin-interface" analysis [6] where the interface thickness W_0 is assumed to be small compared to the scale of the crystal but not smaller than the microscopic capillary length d_0. The phase-field and energy equations were taken from Ref. [7] with the momentum and continuity equations for the liquid taken from Ref. [8]. Furthermore, in the momentum equation, the Lorentz force caused by the alternating electromagnetic field, has been introduced for an undercooled levitated droplet. A system of governing equations is described by

- *energy conservation*

$$\frac{\partial T}{\partial t} + (1-\varphi)(\vec{v}\cdot\nabla)T = a\nabla^2 T + \frac{T_Q}{2}\frac{\partial \Phi}{\partial t}, \qquad (1)$$

- *continuity of the liquid phase*

$$\nabla \cdot \left[(1-\varphi)\vec{v}\right] = 0\,, \tag{2}$$

- *momentum transfer*

$$(1-\varphi)(\vec{v}\cdot\nabla)\vec{v} = -\frac{1-\varphi}{\rho}\nabla p + \frac{(1-\varphi)}{\rho}\vec{F}_{LZ} + \nabla\cdot\left[\frac{\mu}{\rho}\nabla(1-\varphi)\vec{v}\right] + \vec{F}_D\,, \tag{3}$$

- *phase-field evolution*

$$\tau(\vec{n})\frac{\partial\Phi}{\partial t} = \nabla\cdot\left(W^2(\vec{n})\nabla\Phi\right) + \sum_{w=x,y,z}\frac{\partial}{\partial w}\left(\left|\nabla\Phi\right|^2 W(\vec{n})\frac{\partial W(\vec{n})}{\partial(\partial_w\Phi)}\right) - \frac{\partial F}{\partial\Phi}\,. \tag{4}$$

In Eqs. (1)-(4), T is the temperature, T_Q is the adiabatic temperature of solidification defined by $T_Q = Q/c_p$, Q is the latent heat of solidification, c_p is the specific heat, a is the thermal diffusivity, Φ is the phase-field variable ($\Phi=-1$ is for the liquid phase and $\Phi=1$ is for the solid phase); $\varphi=(1+\Phi)/2$ is the fraction of the solid phase ($\varphi=0$ is for the liquid and $\varphi=1$ is for the solid), $\vec{v}$ is the fluid flow velocity in the liquid, x,y,z are the Cartesian coordinates, t is the time, ρ is the density, μ is the dynamic viscosity, and p is the pressure. The dissipative force F_D in the Navier-Stokes equation (3) is taken from Ref. [8]. Furthermore, in the solution of Eq. (3), the Lorentz force has been averaged in time: $F_{LZ} \approx |B|^2/(4\pi\delta)$, where $|B| = B_0 exp[(r-R_0)/\delta]$ is the modulus of the magnetic induction vector, B_o is the time averaged value of the magnetic induction, r is the radial distance of a droplet of radius R_0, $\delta=[2/(\omega\sigma_R\mu_0)]^{1/2}$ is considered as a skin depth for the alternating magnetic field in the droplet, which decreases for a short distance at which the modulus of magnetic induction $|B|$ decays exponentially (where ω is the frequency of the applied current, σ_R is the electric conductivity, and μ_0 is the magnetic permeability). The phenomenological free energy F is defined by $F(T,\Phi)=f(\Phi)+\lambda(T-T_M)g(\Phi)/T_Q$, where T_M is the equilibrium temperature of solidification. With including the double-well function $f(\Phi)=-\Phi^2/2+\Phi^4/4$ and the odd function $g(\Phi)=\Phi-2\Phi^3/3+\Phi^4/5$ itself, the free energy F is constructed in such a way that a tilt λ of an energetic well controls the coupling for T and Φ.

The time $\tau(\vec{n})$ of the phase-field kinetics and the thickness $W(\vec{n})$ of the anisotropic interface are given by

$$\tau(\vec{n}) = \tau_0 a_c(\vec{n}) a_k(\vec{n})\left[1 + a_2\frac{\lambda d_0}{a\beta_0}\frac{a_c(\vec{n})}{a_k(\vec{n})}\right], \qquad W(\vec{n}) = W_0 a_c(\vec{n})\,, \tag{5}$$

where τ_0 is the time scale for the phase-field kinetics, W_0 is the parameter of the interface thickness with $W_0 = \lambda d_0/a_1$, and $a_1 = (5/8)2^{1/2}$. The second term in brackets of Eq. (5) for $\tau(\vec{n})$ defines a correction a_2=0.6267 for the "thin-interface" asymptotic [12]. The anisotropy of interfacial energy is given by

$$a_c(\vec{n}) = \frac{\gamma(\vec{n})}{\gamma_0} = (1-3\varepsilon_c)\left[1 + \frac{4\varepsilon_c}{1-3\varepsilon_c}(n_x^4 + n_y^4 + n_z^4)\right], \tag{6}$$

where $\gamma(\vec{n})$ is the surface energy dependent on the normal vector $\vec{n}$ to the interface, γ_0 is the mean value of the interfacial energy along the interface, and ε_c is the anisotropy parameter. The anisotropy of kinetics of atomic attachment to the interface is given by

$$a_k(\vec{n}) = \frac{\beta(\vec{n})}{\beta_0} = (1+3\varepsilon_k)\left[1 - \frac{4\varepsilon_k}{1+3\varepsilon_k}(n_x^4 + n_y^4 + n_z^4)\right], \tag{7}$$

where $\beta(\vec{n})$ is the kinetic coefficient dependent on the normal vector $\vec{n}$ to the interface, β_0 is the averaged kinetic coefficient along the interface which is defined by $\beta_0 = (1/\mu_{100} - 1/\mu_{110})/(2T_Q)$, and $\varepsilon_k = (\mu_{100}-\mu_{110})/(1/\mu_{100}+1/\mu_{110})$ is the kinetic anisotropy parameter in which μ_{100} and μ_{110} are the kinetic coefficients in the <100>- and <110>-direction, respectively. In Eqs. (5)-(7), the normal vector has the components (n_x,n_y,n_z) defined by the gradients of the phase-field as follows

$$n_x^4 + n_y^4 + n_z^4 = \left[(\partial\Phi/\partial x)^4 + (\partial\Phi/\partial y)^4 + (\partial\Phi/\partial z)^4\right]/|\Phi|^4 .$$

Results and discussion

Equations (1)-(7) have been solved numerically in the three-dimensional space by a finite-difference technique on a uniform computational grid. We used a multi-grid algorithm for resolving the equations of the phase-field (4), heat transfer (1) and momentum (3) which have different spatial lengths and time scales of their dynamics. Parameters of modeling and material parameters for pure nickel are given in Refs. [5,9].

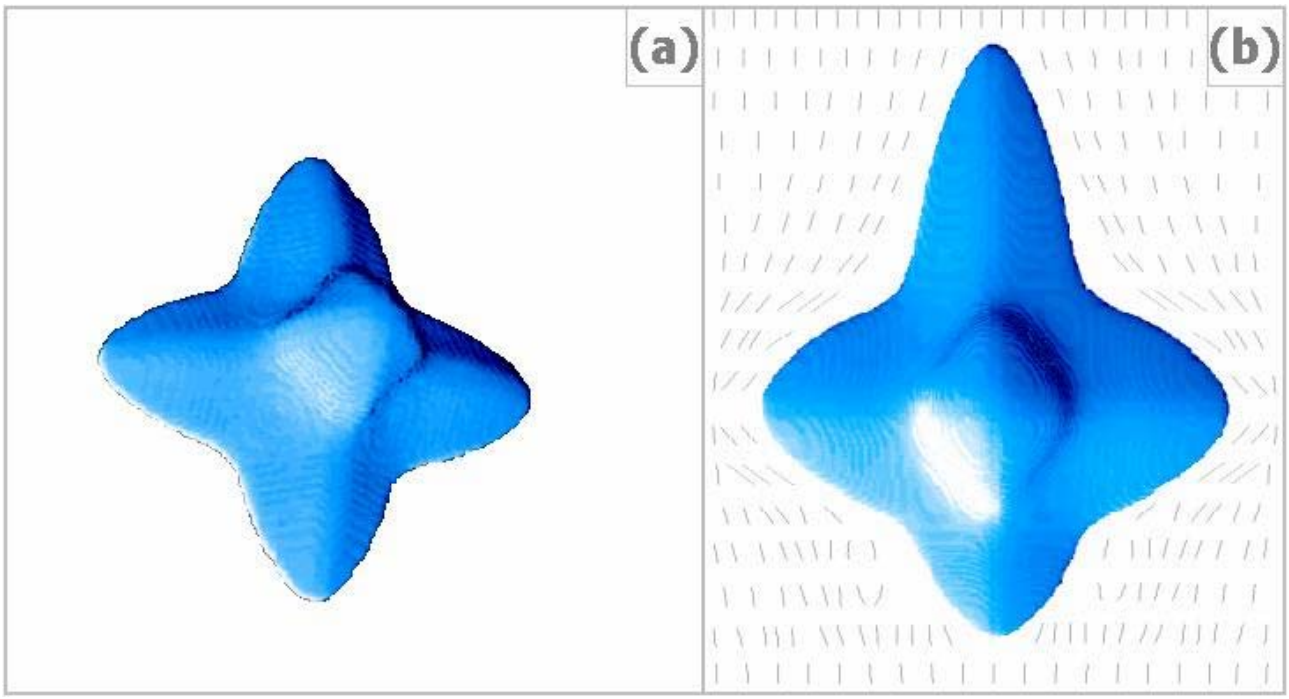

Figure 1. (a) Dendritic pattern growing into a stagnant pure nickel melt at the undercooling ΔT=0.30T_Q (K). The pattern has been simulated using a grid of size 450^3 nodes. The details of modeling are given in Ref. [9]. (b) Growth of nickel dendrite under convective flow at the undercooling ΔT=0.30T_Q (K) and the fluid flow velocity U_0=0.7 (m/s) imposed at the top surface of the computational domain. The growth velocity of the up-stream branch is pronounced in comparison with the down-stream branch due to forced convection. Dashed lines around the dendrite indicate the flow velocity vectors in the vertical cross-section. The pattern has been simulated using a grid of size 230×230×330 nodes.

Dendritic patterns. We obtained the morphological spectrum of interfacial crystal structures for a wide range of undercoolings. In our modeling, the spectrum of the obtained crystal structures exhibits a change from grained crystals at very small undercoolings ($\Delta T<0.15T_Q$) to dendritic patterns at intermediate undercoolings ($0.1T_Q<\Delta T<1.0T_Q$) to grained crystals again at high undercoolings ($\Delta T>1.0T_Q$). Within the range of intermediate undercoolings, the shape of dendrites is dictated by the preferable crystallographic direction (which is the <100> direction for the case of Ni). Figure 1(a) shows the dendritic crystal whose growth has been dictated by the preferable crystallografic directions (these are the <100> directions for nickel for all ranges of undercooling). Solidification under the influence of forced convective flow in a droplet produces dendritic growth that is pronounced in the direction opposite to that of the far field flow velocity U_0 (see Ref. [4]). The present results of modeling also confirm this outcome: with imposing the fluid flow, the growth becomes pronounced in the direction opposite to the flow as shown in Fig. 1(b). For these structures, i.e. growing in a stagnant melt and also with the melt flow (Fig. 1) we compared the results for dendrite growth velocity V in pure Ni versus undercooling ΔT quantitatively.

The results of phase-field modeling exhibit an increase of the velocity of the up-stream dendrite branch, Fig. 1(b). When the thermal boundary layer shrinks ahead of the up-stream branch due to the flow, the heat of solidification is removed faster, and the growth velocity enhances. The enhanced dendrite velocity due to the melt flow decreases the discrepancy between theory and experimental data at small undercoolings. Hence we have compared the predictions of the present phase-field modeling with the new experimental data [5] for growth kinetics of nickel dendrites.

Comparison with experimental data. In comparison with the experimental measurements summarized in Ref. [1], we improved the accuracy of the technique and performed new measurements of dendritic growth velocities in levitated nickel samples [5]. The measurements were performed for the dendritic growth velocity V as a function of undercooling $\Delta T=T_L-T_\infty$, measured experimentally for the melted drop (T_L is the liquidus temperature, and T_∞ is the actual temperature of the drop). Solidification of the melt was triggered in the range of 30 K<ΔT<260 K.

Comparison of these new data with the solution of Eqs.(1)–(7) confirms that convection alone cannot describe the experimental results satisfactorily. An additional reason for the remaining discrepancy might be due to the presence of small amounts of impurities [5]. Therefore, we have used the sharp-interface model [10] to evaluate the influence of the solute diffusion on dendrite growth kinetics. As it can be seen in Fig. 2, the dendrite tip radii for pure Ni and, respectively, for Ni with impurities differ significantly (the details of computation will be published elsewhere [11]). E.g., for Ni with 0.01 at.% of impurity, the transition from solute diffusion-limited growth to the 3 by de h

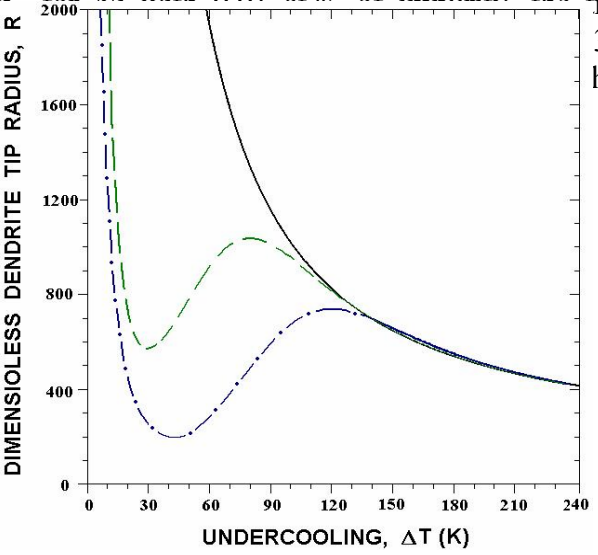

Figure 2. Dendrite tip radius as a function of undercooling. The solid line is for pure Ni, the dashed line is for Ni with 0.01 at. % of impurity, and the dashed-dotted line is for Ni with 0.05 at.% of impurity.

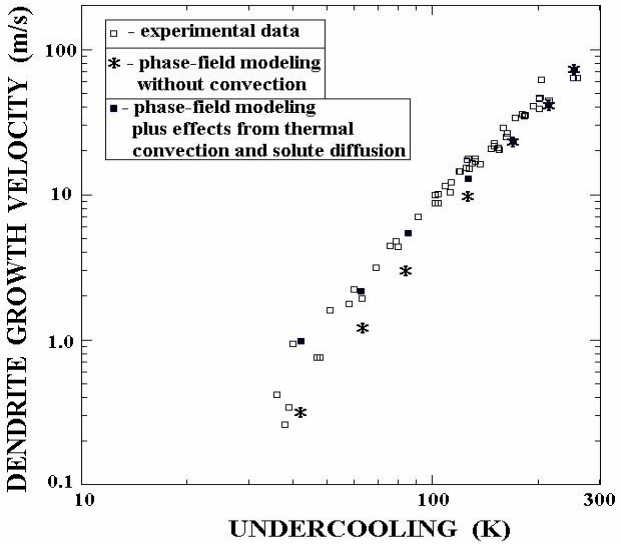

Figure 3. Comparison of data from experiment (open squares), phase- field modeling for pure Ni without with flow (stars), and final data (black squares) with the effect from thermal convection and solute diffusion.

Consequently, we have found that small amounts of impurities in nickel can lead to an enhancement of the growth velocity but with a temperature characteristic different from that of the effect of fluid flow. This allows to discriminate between both contributions and model them separately by means of the phase-field modeling of dendritic solidification with convective flow and the sharp-interface model of dendritic growth of a binary system. Therefore, using the results of the present phase-field modeling for pure nickel, Eqs. (1)-(7), and the sharp-interface model [10] for Ni + 0.01 at.% of impurity, we determined the final growth velocity as follows:

$$V(\Delta T) = V_{Ni}(\Delta T) + V_{Conv}(\Delta T) + V_{Dif}(\Delta T),$$

where $V_{Ni}(\Delta T)$ is the velocity obtained from the phase-field modeling without convection of the liquid phase, $\Delta V_{Conv}(\Delta T)$ is the increase in velocity due to convection estimated from the phase-field modeling with convection, and $\Delta V_{Dif}(\Delta T)$ is the increase in velocity due to presence of a small amount of impurity obtained from the sharp interface model. The increases $\Delta V_{Conv}(\Delta T)$ and $\Delta V_{Dif}(\Delta T)$ were computed relatively to the velocity $V_{Ni}(\Delta T)$ given by the phase-field modeling of dendrite solidification without convective flow. Figure 3 shows the final comparison of the modeling data and experimental results for the growth velocity of nickel dendrites. It can be seen that we obtain good agreement with the experimental data provided both convection and solute diffusion are taken into consideration.

Conclusions

The results of the phase-field model lead to the conclusion that forced convective flow enhances the growth velocity in the range of small undercoolings where the dendrite growth velocity is comparable to the velocity of the flow. Using the sharp interface model [10], it is shown that even small amounts of impurities on the level of 0.01 at. % lead to an enhancement of the growth velocity in the range of small and intermediate undercoolings. The solute effect, however, shows a different temperature characteristics than the transport effect by fluid flow, which makes it possible to discriminate between both these effects by investigating the dendritic growth velocity V as a function of undercooling ΔT.

Acknowledgements

The authors thank Prof. Wilfried Kurz and Prof. Christoph Beckermann for stimulating discussions and useful exchanges. Financial support of this work by Deutsche Forschungsgemeinschaft under the project No. HE 1601/13 is gratefully acknowledged.

References

[1] K. Eckler, D.M. Herlach, Mater. Sci. Eng. A **178** (1994) 159.

[2] D.M. Matson, in: *Solidification 1998*, edited by. S.P. Marsh, J.A. Dantzig, R. Trivedi, W. Hofmeister, M.G. Chu, E.J. Lavrenia, J.-H. Chun (TMS, Warrendale PA, 1998) p. 233.

[3] J. Lipton, W. Kurz, R. Trivedi, Acta Metall. **35** (1987) 957.

[4] P.K. Galenko, O. Funke, J. Wang, D.M. Herlach, Mater. Sci. Eng. A **375-377** (2004) 488.

[5] O. Funke, G. Phanikumar, P.K. Galenko, M. Kolbe, D.M. Herlach, J. Appl. Phys. (2004) *submitted*.

[6] A. Karma, W.-J. Rappel, Phys. Rev. E **57** (1998) 4323.

[7] J. Bragard, A. Karma, Y. H. Lee, M. Plapp, Interface Science **10** (2002) 121.

[8] C. Beckermann, H.-J. Diepers, I. Steinbach, A. Karma, X. Tong, J. Comp. Phys. **154** (1999) 468.

[9] B. Nestler, D. Danilov, P. Galenko, J. Comp. Phys. (2004) *submitted*.

[10] P.K. Galenko, D.A. Danilov, Phys. Lett. A **235** (1997) 271.

[11] P.K. Galenko, D.M. Herlach, G. Phanikumar, O. Funke, Phase-field modeling of solidification of undercooled melt: a test and comparison for the current models with the new experimental data. *Manuscript in preparation* (2004).

Solidification and Gravity IV
doi:10.4028/www.scientific.net/MSF.508

Phase-Field Modeling of Dendritic Solidification in Undercooled Droplets Processed by Electromagnetic Levitation
doi:10.4028/www.scientific.net/MSF.508.431